Local epidemiology of the wood decay agent Laetiporus sulphureus in carob stands in Sicily

Local epidemiology of the wood decay agent *Laetiporus sulphureus* in carob stands in Sicily

Fabiano Sillo[1], Carmelo Gianchino[2], Luana Giordano[1,3], Marta Mari[2], and Paolo Gonthier[1*]

[1]*University of Torino, Department of Agricultural, Forest and Food Sciences, Largo Paolo Braccini 2, I-10095 Grugliasco, Italy.*

[2]*University of Bologna, Department of Agricultural Sciences, Viale Fanin 46, I-40127 Bologna, Italy.*

[3]*University of Torino, Centre of Competence for the Innovation in the Agro-Environmental Field (AGROINNOVA), Largo Paolo Braccini 2, I-10095 Grugliasco (TO), Italy.*

[*]Corresponding author: paolo.gonthier@unito.it

Summary

The basidiomycete *Laetiporus sulphureus* (Bull) Murrill is a forest pathogen causing brown cubical heart rot in a broad range of host trees. Despite its wide distribution and importance, studies aimed at understanding the epidemiology of the fungus in specific areas or hosts are lacking. In this study, an incidence of *L. sulphureus* as high as 34% was determined through molecular analysis of wood samples collected from 70 carob (*Ceratonia siliqua* L.) trees in the South West of Sicily, Italy. A phylogenetic analysis of Internal Transcribed Spacer (ITS) sequences indicated that all carob isolates belonged to the cluster E of *Laetiporus* taxonomy. Ten molecular markers based on Single Sequence Repeats (SSRs) designed on the *L. sulphureus* genome were developed and isolates were genotyped through High Resolution Melting (HRM) analysis. High gene diversity (0.581), no correlation between fungal genotype and host tree species and significant correlation between spatial and genetic

distance were observed, suggesting an important role of basidiospores in the epidemiology of the fungus and a risk of transmission from a host tree species to the others. Finally, from a prognostic perspective, significant differences among isolates in terms of mycelial growth suggest that in addition to an accurate identification, a phenotypic characterization of isolates affecting trees may also be important.

Introduction

The genus *Laetiporus* Murril (Polyporales) includes wood-rotting basidiomycetes growing on a wide variety of broadleaf and conifer trees (Bernicchia, 2005). The origin and biogeography of the genus has been resolved only recently (Song & Cui, 2017). Currently, it is recognized that the genus *Laetiporus* comprises eleven species and four undescribed worldwide distributed taxa (Gilbertson & Ryvarden, 1986; Song & Cui, 2017), including *L. ailaoshanensis* B.K. Cui & J. Song, *L. caribensis* Banik & D.L. Lindner, *L. cincinnatus* (Morgan) Burds., Banik & T.J. Volk, *L. cremeiporus* Y. Ota & T. Hatt., *L. conifericola* Burds. & Banik, *L. gilbertsonii* Burds, *L. huroniensis* Burds. & Banik, *L. montanus* Černý ex Tomšovský & Jankovský, *L. sulphureus* (Bull) Murrill, *L. versisporus* (Lloyd) Imazeki, and *L. zonatus* B.K. Cui & J. Song (Song & Cui, 2017).

L. sulphureus is one of the most studied species of the genus. The edible shelf-shaped, pink-orange to yellow fruiting bodies of *L. sulphureus* are indeed a rich source of antioxidant and antimicrobial compounds, including polysaccharides, hemolectins and laetiporic acids used in pharmaceutical and industrial processes (Turkoglu et al., 2007; Petrović et al., 2013). In addition, fruiting bodies also contain α-1-3-glucans, which are used as inducers of bacterial mutanases, i.e. enzymes involved in the degradation of biofilms formed by the etiologic agents of dental caries (Wiater et al., 2012). The nutritional and pharmaceutical values of *L. sulphureus* fruiting bodies (Petrović et al., 2014) led to significant efforts for the development of cultivation methods of this fungus at the industrial scale

(Pleszczyńska et al., 2013).

However, *L. sulphureus* is also a forest pathogen (Schwarze, Engels, & Mattheck, 2000; Dai et al. 2007). As an important wood decay agent, it infects a broad range of hosts both in forests and urban areas, including *Castanea sativa* L., *Eucalyptus* spp., *Fagus* spp., *Quercus* spp., *Populus* spp., *Prunus* spp., *Pyrus* spp., *Robinia* spp., *Salix* spp., and occasionally *Tilia* spp. (Schwarze, Engels, & Mattheck, 2000; Bernicchia, 2005; Giordano et al., 2015). Infection is hypothesized to occur by means of basidiospores germinating on injured bark of stems or roots (Schwarze, Engels, & Mattheck, 2000). The fungus colonizes the wood through the libriform fibers by breaking down the cellulose (Schwarze, Engels, & Mattheck, 2000). The stem decay columns can be 5-8 meters long and are generally associated with heartwood (Bernicchia, 2005). Sapwood may also be invaded, but only in the root systems (Schwarze, Engels, & Mattheck, 2000). After the establishment into the tree, sexual reproduction may occur in fruiting bodies emerging outside the trunk (Bernicchia, 2005). Furthermore, being a necrotrophic parasite, *L. sulphureus* is able to colonize dead trees and stumps as a saprotroph (Schwarze, Engels, & Mattheck, 2000).

Research on *L. sulphureus* was mostly focused on the development of protocols to cultivate the mycelia (Pleszczyńska et al., 2013), on the characterization of the plethora of compounds in the fruiting bodies (Petrović et al., 2013), and on resolving the puzzling phylogenesis of the species and related taxa (Song & Cui, 2017). For example, somatic incompatibility assays, allozyme and, more recently, multi-locus phylogenetic analyses allowed mapping the different *Laetiporus* taxa in Europe, North America and Asia (Banik & Burdsall Jr, 2000; Lindner & Banik, 2008, 2011; Vasaitis et al., 2009; Song et al., 2014). Comparative phenotypic assays *in vitro* further supported and confirmed the differentiation among species (Vasaitis et al., 2009).

However, studies aimed at understanding the epidemiology of *L. sulphureus* in specific areas or hosts are lacking, with a very few exceptions (Rogers, Holdenrieder, & Sieber, 1999). The main issue is that, although *L. sulphureus* can be easily found in natural ecosystems in North America and Europe (Vasaitis et al., 2009), sites where fungal fruiting bodies are abundant are rare. In South West of Sicily

92 (Italy), *L. sulphureus* appears to be associated with carob trees (*Ceratonia siliquia* L.) (Bernicchia,
93 2005). In the past, carob was considered a profitable tree species in Sicily, since its pods were
94 consumed as food and used to feed livestock (Barbagallo et al., 1997). Currently, carob is regaining
95 importance as ornamental and forest tree in marginal areas and because of the industrial use of its
96 pods (La Malfa et al., 2014). In the complex phytosanitary conditions of carob, which can be affected
97 by several plant pathogens and pests (Ramon-Laca & Mabberley, 2004; Vannini et al., 2017), a
98 relevant role is played by stem decays caused by *L. sulphureus* (Battle & Tous, 1997). The abundance
99 of *L. sulphureus* fruiting bodies on carob trees in the area of Modica and Ragusa, South West of Sicily,
100 makes this area an excellent sampling site for epidemiological studies. The aims of this work were:
101 I) to determine the incidence of *L. sulphureus* on carob trees in a selected area in Sicily, II) to develop
102 molecular markers to elucidate the genotypic and allelic diversity of *L. sulphureus* in this area, III) to
103 perform an analysis of the phenotypic diversity of *L. sulphureus*, through *in vitro* growth assays, and
104 IV) to explore the relationship between *in vitro* growth levels of mycelia and genotypic diversity.
105

106 ## Materials and methods

107

108 **Sampling sites, wood and fungal materials**

109 To estimate the incidence of *L. sulphureus* in carob trees, the sampling area comprised about 270 km^2
110 in Modica Municipality (South West of Sicily, Italy) (Figure 1). A total of 70 randomly selected
111 standing carob trees were sampled in December 2015. Trees were about 80 years old and
112 characterized by a Diameter at Breast Height (DBH) ranging from 55 to 80 cm. Twenty-four trees
113 showed symptoms of wood decay, i.e. discoloration of exposed wood in pruning wounds or cracks,
114 while 46 trees did not show any mechanical damage, nor visible wood decay or crown symptoms.
115 These 46 trees were regarded as asymptomatic. *Laetiporus* fruiting bodies were neither observed on
116 the sampled trees nor on the neighbouring trees. Each tree was drilled four times (drillings at 90°
117 from one another) 50 cm aboveground according to a previously described sampling protocol

(Guglielmo et al., 2010). Wood chips generated from different drillings of the same tree were pooled together as a single sample in a 90-mm Petri dish and lyophilized overnight (Guglielmo et al., 2010). For phylogenetic, genetic and phenotypic analyses, *L. sulphureus* fruiting bodies were collected during Summer 2016 (June-August 2016) in a broader area in South West of Sicily (Figure 1). In detail, 24 fruiting bodies were collected from carob trees and one from an almond tree (*Prunus amygdalus* Batsch). Distance between the trees from which fruiting bodies were collected ranged between 0.5 to 35.4 km. Four additional fruiting bodies collected in Northern Italy were included in the genetic analysis as outgroups, three of these originating from European chestnut (*Castanea sativa* L.) and one from oak (*Quercus* sp.). Altogether 29 fruiting body samples were processed (Table 1). Isolates were obtained from fruiting bodies by placing fragments of tissues (approximately 2 x 2 x 1.5 cm in size) excised from the context in 90-mm Petri dishes containing Malt Extract Agar and citric acid (MEA; malt extract agar 33.6 g/L, citric acid 0.5 g/L). Isolates were incubated at 25°C±2°C for one week and subsequently sub-cultured in 250-mL flasks, filled with Malt Extract liquid medium (2% w/v) in the dark at 25°C±2°C for a week before being harvested for DNA extraction.

Molecular detection of *L. sulphureus* in wood samples

About 200 mg of lyophilized wood chips per sample were homogenized with the aid of glass beads (3 mm and 5 mm) in a FastPrep FP120 Cell Disrupter (Qbiogene, Irvine, CA, USA). DNA extraction from wood samples was performed by using the E.Z.N.A.™ Stool DNA Isolation Kit (Omega Bio-Tek, Doraville, CA, USA). Taxon specific primers developed by Guglielmo et al. (2007) were used in PCR to identify samples positive to *L. sulphureus* s.l. PCR assays were performed in a 25 µl volume containing 5x of PCR buffer, 1.5 mM of $MgCl_2$, 0.2 mM of dNTPs mix, 0.5 µM each of the taxon specific primers, 0.025 U/µl of GoTaq® polymerase (Promega, Madison, WI, USA) and 6.25 µl of the 50-fold dilution of the DNA extracted from wood (Guglielmo et al., 2007). PCR reactions were performed using an initial denaturation at 94°C for 3 minutes, followed by 35 cycles with each cycle consisting of a denaturation at 94°C for 30 seconds, an annealing at 60°C for 45 seconds, an extension

144 at 72°C for 1 minute, and one final extension cycle at 72°C for 10 minutes. The presence of amplicons
145 in samples were checked, after electrophoretic migration (6 V/cm) on a gel containing 1.5% (w/v) of
146 agarose, through the use of the Image Lab™ Software (Bio-Rad Laboratories, Hercules, CA, USA).
147
148 **Phylogenetic analysis of *L. sulphureus* isolates**
149 Mycelia from the 29 isolates were dried overnight with a lyophilizer equipped with a vacuum pump.
150 About 200 mg of dried mycelia per sample were homogenized by using glass beads (diameter 2 mm
151 and 4 mm) in a FastPrep FP120 Cell Disrupter (Qbiogene, Irvine, CA, USA). Total DNA extraction
152 was performed using DNeasy Plant Mini Kit (Qiagen Inc., Valencia, CA, USA), following
153 manufacturer instructions. The DNA samples were used as templates for PCRs with the primer pair
154 ITS1F/ITS4, which amplifies the Internal Transcribed Spacer (ITS) regions of the fungal nuclear
155 ribosomal RNA gene (nrDNA; Gardes & Bruns, 1993). The PCR mix included 6.25 µL of DNA, 0.75
156 U of GoTaq polymerase (Promega, Madison, WI, USA), 0.5 µM of each primer, 200 µM of each
157 dNTP, and 5 µL of the 5x buffer in a total volume of 25 µL. The PCR protocol was as follows: an
158 initial denaturation step at 94°C for 3 minutes, followed by 35 cycles at 94°C for 30 seconds, 54°C
159 for 30 seconds, and 72°C for 45 seconds, and a final elongation step at 72°C for 10 minutes.
160 Amplicons were visualized on 1% (w/v) agarose gel after electrophoresis at 6 V/cm for 30 minutes.
161 PCR products were purified by using ExoSAP-IT (Affymetrix, Santa Clara, CA, USA) at 37°C for
162 15 minutes followed by 80°C for 15 minutes. The purified PCR products were sequenced at BMR
163 Genomics S.r.l. (Padua, Italy). A multiple sequence alignment was built using the ClustalW algorithm
164 inside MEGA version 6 (Tamura et al., 2013). Phylogenetic trees were constructed using the
165 Maximum Likehood (ML) method (Jukes-Cantor model), with the MEGA v. 6 software. Bootstrap
166 analyses were carried out on the basis of 100 re-samplings of the sequence alignment. A total of 78
167 *Laetiporus* spp. nucleotide sequences deposited in GenBank from previous phylogenetic studies by
168 Vasaitis et al. (2009) and by Song & Cui (2017) were also included in the phylogenetic analysis.
169 Representative ITS nucleotide sequences from the present study were deposited in the GenBank

database under the accession numbers MG386383- MG386385.

Development of SSR-based markers, HRM genotyping and analysis of genetic diversity of isolates

MSDB 2.4.2 (Microsatellite Search and Database) (Du et al., 2013) was used to scan the entire *L. sulphureus* genome (*Laetiporus sulphureus* var. *sulphureus* v1.0; Nagy et al., 2015) to search for perfect Single Sequence Repeats (SSRs), using the "perfect" search mode. Six classes of microsatellites were detected as follows: mono-, di-, tri-, tetra-, penta- and hexa-nucleotide SSR motifs with minimum repeat number of 12, 7, 5, 4, 4, 4, respectively. Five mono-, four di-, nine tri-, one tetra- and one hexa-nucleotide SSRs were selected as candidate marker regions, based on length of SSR motifs (minimum length 10 repeats) and GC-content above 60% in the flanking regions, this totalling 20 SSR markers. The design of specific primer sets to amplify SSR loci was performed by using Primer3Plus (http://www.bioinformatics.nl/cgi-bin/primer3plus/primer3plus.cgi/). Each primer pair was tested in PCR on DNA of the isolates VALLERE and C2 (Table 1), and the presence of amplification products was checked by agarose electrophoresis.

All the isolates were subjected to PCR with the verified primer pairs, coupled with High Resolution Melting (HRM) analysis, to identify polymorphic loci and to determine isolate specific allelic variation at such loci. The DNA of each sample was quantified by using the NanoDrop (Thermo Scientific, Wilmington, DE, USA) in order to use a standard concentration of template DNA in PCR reactions. The PCR for the HRM analysis was carried out with Connect™ Real-Time PCR Detection System (Bio-Rad Laboratories, Hercules, CA, USA). Each PCR reaction was conducted on a total volume of 10 µl, containing 1 µl of appropriately diluted DNA (20 ng/µl), 5 µl Sso Fast Eva Green Supermix (Bio-Rad Laboratories, Hercules, CA, USA), 0.3 µl of each primer (3 µM) and 3.4 µl of water, using a 96 well plate. The following PCR programme, which included the calculation of a melting curve, was used: 98°C for 2 minutes, followed by 45 cycles of 98°C for 10 seconds and 59°C for 20 seconds, and terminated by ramp from 65°C to 95°C with a temperature increment of 0.1°C

196 and a plate read every 10 seconds. Melting curves were analysed by using the Precision Melt
197 Analysis™ Software from Bio-rad, setting the Tm difference threshold at 0.15 and the Melt curve
198 shape sensitivity at 50. This software allowed to group the melting curves in different clusters,
199 representing different alleles of SSR loci. By analyzing the melting curves, alleles were assigned to
200 all isolates for each SSR locus and a matrix including all the allelic data obtained was prepared.
201 Number of observed alleles *per* locus (Na), number of effective alleles based on their frequencies
202 (Ne) and gene diversity (*h*) were estimated from the data matrix using the software GenAlEx version
203 6.5 (Peakall & Smouse, 2012). The software was also used for calculating the overall observed and
204 expected levels of heterozygosity based on the number of melting curve peaks and effective number
205 of alleles detected *per* locus, respectively.
206
207 ***In vitro* growth assays and phenotypic diversity of isolates**
208 Growth assays were performed by inoculating a plug of mycelium (6 mm in diameter) obtained from
209 the margin of actively growing cultures of each Sicilian isolate on the centre of 90-mm Petri dishes
210 containing MEA. Five replicates for each isolate were prepared and Petri dishes were incubated at
211 25°C±2°C in the dark. The extent of fungal colonization in mm was measured every 48 hours until
212 the mycelia reached the edges of the Petri dish. Two perpendicular measures of radial growth for each
213 replicate were taken. Observations on the colony pigmentation were conducted on 8-days old pure
214 cultures of Sicilian isolates grown at 25°C on Petri dishes filled with MEA.
215
216 **Statistical analyses**
217 The software GeneAlEx version 6.5 was used to perform the Principal Coordinates Analysis (PCoA)
218 on both genetic (matrix of genetic distances between isolates) and phenotypic (matrix obtained from
219 pairwise comparison of growth curves) data matrices. The same program was used to assess the
220 minimum number of SSR loci needed to discriminate all genotypes, through a genotype accumulation
221 curve of multi-locus match probability for increasing combinations of loci. The XLSTAT© software

222 package (Addinsoft, Paris, France) was used to assess the association between spatial and genetic
223 distances, by performing Spearman's rank correlation test. The XLSTAT© software package was also
224 used to assess the association between genetic distance and growth coefficients pairwise by
225 performing the Spearman's rank correlation test. Significant ($p < 0.05$) differences among isolates in
226 terms of growth *in vitro* were assessed by using the *compareGrowthCurves* function
227 (http://bioinf.wehi.edu.au/software/compareCurves/) from the R Statistical Modeling package
228 *statmod*. This function performed permutation tests (1000 permutations) of the differences between
229 groups in growth rate.
230

231 ## Results

232

233 **Incidence of *L. sulphureus* in carob trees**

234 The use of taxon-specific primers detected *L. sulphureus* in 24 samples out of 70, corresponding to a
235 34.28% incidence. The positive samples, showing a typical band of 146 bp, were obtained from 11
236 trees showing symptoms of decay and from 13 asymptomatic trees.
237

238 **Phylogenetic analysis of *L. sulphureus* isolates**

239 Phylogenetic analysis based on ITS sequences of *Laetiporus* spp. included the now generated ITS
240 sequences and ITS sequences of reference *Laetiporus* spp. from different geographic origins and
241 different hosts. In the first phylogenetic tree, the 25 Sicilian isolates clustered inside the cluster E: 17
242 grouped in the sub-cluster E1, and seven in the sub-cluster E2 (Figure 2). The ITS sequence of isolate
243 C1 showed five additional SNPs compared to the other isolates and was considered as belonging to
244 E1. The four additional Italian isolates grouped in the sub-cluster E2 (Figure 2). In the second
245 phylogenetic tree, which included only isolates of *L. sulphureus*, the Italian isolates grouped in the
246 cluster E, which contained isolates obtained from different host trees, i.e. *Eucalyptus* sp., *Fraxinus*

247 sp., *Prunus* sp. and *Quercus* sp., in addition to those from carob (Figure 3).

248

249 **Development of SSR-based markers, HRM genotyping and analysis of genetic diversity of**
250 **isolates**

251 Eleven out of 20 tested SSR markers were amplifiable through PCR and hence were used in the HRM
252 genotyping. One locus turned out to be monomorphic as it showed no variation in melting curves
253 between the samples and hence it was excluded from analysis. The remaining ten SSR markers were
254 polymorphic based on HRM analysis, showing a minimum of two alleles (locus Ls_GGA_174) and
255 a maximum of ten alleles (locus Ls_ATGCCC_111) (Figure 4). Primers developed and used to
256 amplify the polymorphic SSR markers are reported in Table 2.

257 Melting curve difference plots for the ten polymorphic loci are visualized in Figure 4. Number of
258 alleles and number of effective alleles based on allele frequencies for each locus are reported in Table
259 2. All SSR loci analysed in this study were homozygous in all isolates, with the exception of locus
260 Ls_AC_322 for which isolates F3 and F6 showed a typical double peak in the melting curve plots,
261 suggesting a heterozygous condition (Figure S1) at this locus. For this locus, these two isolates were
262 grouped in a separate cluster/allele in the subsequent HRM analysis. The observed and expected
263 levels of heterozygosity were 0.007 and 0.581, respectively. Average gene diversity (*h*) was 0.581 (±
264 0.079). The HRM genotyping identified 29 genotypes out of 29 isolates. Multilocus matches by locus
265 for increasing combinations of all the ten loci showed that the minimum number of SSR markers
266 allowing distinction between all isolates was nine.

267 The PCoA based on genetic data did not show distinct groups (Figure 5). The percentage of variation
268 explained by the first two axes was 34.68%. A slight distinction between isolates belonging to E1 and
269 E2 sub-clusters was observed, with the exception of isolate C1 (Figure 5). The isolates obtained from
270 chestnut (GAIOLA, Em-a, Em-b), oak (VALLERE) and almond (G5) grouped together with the other
271 isolates (Figure 5). The Spearman's rank correlation test between pairwise genetic and geographical
272 distances within the 25 Sicilian isolates showed a significant positive correlation (0.142, *p*-value =

273 0.014).

274

275 **Growth assay *in vitro* and analysis of phenotypic diversity**

276 Mycelial growth assessed *in vitro* showed that six isolates (C2, D4, D5, O2, O3 and F5) were able to
277 fully colonize the Petri dish in 6 days only (Table 3). Isolates C1, C4 and F1 did not reach the edge
278 of the Petri dish after 8 days (Table 3). PCoA on mycelial growth data allowed to distinguish four
279 different groups: one group representing the fastest growing isolate O3, two intermediate groups
280 including 10 and 12 isolates, respectively, and a group including the isolates C1 and F1 characterized
281 by low growth (Figure 6). The percentage of variation explained by the first two axes was 66.41%.
282 Statistical analysis performed with *compareGrowthCurves* function showed significant differences
283 among the four clusters identified (p-value < 0.05). The Spearman's rank correlation test between
284 pairwise genetic distances and pairwise mycelial growth coefficients showed no significant
285 correlation (p-value > 0.05).
286 A slight difference in pigmentation between Sicilian isolates was observed. In particular, 11 isolates
287 (C1, C3, D3, D5, F1, F4, F5, G4, G5, O1 and O3) showed white mycelia, while the remaining 14
288 isolates (C2, C4, D1, D4, F2, F3, F6, G1, G2, G3, G6, G7, I1 and O2) showed yellow-to-orange
289 mycelia.

290

291 ## Discussion

292

293 This epidemiological study on *L. sulphureus* associated with carob trees has provided insights into
294 the presence and the distribution of this wood decay agent in the South West of Sicily. In this work,
295 34% of the sampled trees were found to be infected by *L. sulphureus*, based on molecular detection.
296 The high occurrence frequency of this species, generally diagnosed based on the inspection of visible
297 fruiting bodies, implies that the prevalence of this species is largely underestimated as previously
298 observed in surveys conducted in urban areas (Giordano et al., 2015). None of the sampled carob

299 trees showed visible fruiting bodies, which may be partly due to the period of sampling (i.e.
300 December). The majority of trees (66%) did not show any external symptoms of wood decay either.
301 From an ecological perspective, *L. sulphureus* has long been regarded as belonging to the group of
302 true heart rots colonizing heartwood exposed by natural injuries (Vasiliauskas, Sunhede, & Stenlid,
303 2003; Vasaitis, 2013). The now observed prevalent incidence of *L. sulphureus* in asymptomatic carob
304 trees might suggest that the fungus could be considered as a true heart rot of intact tree stems, when
305 following the classification of Vasaitis (2013). However, it should be noted that unravelling the
306 ecological strategies of *L. sulphureus* was beyond the scope of our study. Further research with an
307 experimental design tailored for the purpose is needed to understand whether *L. sulphureus* may
308 belong to the category of true heart rots of intact tree stems, which would imply an ability to colonize
309 trees without wounding.
310 The widespread presence of *L. sulphureus* on carob trees may have been favoured by the
311 abandonment of cultivation of this tree species in the area. In the recent past, carob pods prices
312 dramatically decreased, making the cultivation of carob trees no longer economically profitable
313 compared to other crops, such as vineyards (Barbera & Cullotta, 2012). The cultivation of this woody
314 crop has indeed radically decreased from about 70,000 ha during the 60's to less than 30,000 ha by
315 early 21st Century (Massa & La Mantia, 2007). As a consequence, the abandonment of agricultural
316 practices on Sicilian carob trees, such as removal of decayed wood residuals, may have favoured the
317 establishment and spread of *L. sulphureus* in this area.
318 The prevalent presence of *L. sulphureus* fruiting bodies on several trees in the Modica municipality
319 allowed to perform a genetic diversity analysis of this pathogen in the area. Previous phylogenetic
320 analyses on ITS region of *Laetiporus* isolates from different countries have showed that the species
321 *L. sulphureus* includes at least two distinct clusters, C and E (Vasaitis et al., 2009; Song et al., 2014).
322 The cluster C included European isolates only, while cluster E comprised isolates originating from
323 different European, South American, and North American countries (Vasaitis et al., 2009). Our
324 phylogenetic analysis showed that all Italian isolates grouped within the cluster E. Seventeen isolates

325 from South Western Sicily were grouped in the sub-cluster E1, while the remaining 12 isolates,
326 including isolates from other Italian regions, i.e. Tuscany and Piedmont, clustered in the sub-cluster
327 E2. These two sub-clusters were previously defined on the basis of phenotypical observations, i.e.
328 colours of the fruiting body pores (white or yellow) (Burdsall Jr & Banik, 2001; Song et al., 2014).
329 Our phylogenetic analysis on ITS regions confirmed the absence of a link between cluster and host
330 species, as previously observed (Vasaitis et al., 2009). Isolates obtained from fruiting bodies collected
331 from carob trees, European chestnuts, oak and almond clustered together with other European isolates
332 collected from different host plants, such as ashes and eucalypts.
333 In order to increase the resolution of genetic characterization, novel molecular markers specific for
334 *L. sulphureus* were developed, by using large scale genomic data (Nagy et al., 2015). SSR-based
335 markers are widely used and popular due to their high reproducibility and multiallelic nature, and
336 their power for genetic characterization of populations of wood decay fungi has been demonstrated
337 (Franzen et al., 2007; Travadon et al., 2012; Maurice et al., 2014; Gonthier et al., 2015). The analysis
338 of SSRs coupled with HRM is a robust and reproducible method (Ganopoulos, Argiriou, & Tsaftaris,
339 2011), as it has been successfully used in genotyping of plants (Xanthopoulou et al., 2014; DiStefano
340 et al., 2012), and, more recently, of fungal pathogens (Zambounis et al., 2016; Sillo et al., 2017). The
341 HRM genotyping of the ten SSR markers allowed to distinguish all isolates from one another. In
342 addition, this analysis allowed detection of heterozygous allelic conditions, often observed in
343 heterokaryotic basidiomycetes (Nazrul & YinBing, 2011), yet uncommon in the *L. sulphureus* isolates
344 analysed in this study. The relatively high number of observed alleles *per* locus and the high gene
345 diversity (0.581) are not in disagreement with the hypothesis that *L. sulphureus* retains high allelic
346 recombination due to sexual reproduction (Milgroom, 1996), although the fungus is also known to
347 develop an asexual stage (Stalpers, 1978; Bernicchia, 2005). However, the observed level of
348 heterozygosity was substantially lower than the expected one, which might indicate that *L.*
349 *sulphureus*, or at least the studied population, is homothallic, a condition previously suggested for
350 other *Laetiporus* taxa, but not for *L. sulphureus* (Banik & Burdsall Jr, 2000; Banik et al., 2010).

351 The PCoA of genetic data did not divide the samples into distinct groups, but there was a slight
352 differentiation between isolates from sub-cluster E1 and E2. Interestingly, the genotype C1, belonging
353 to sub-cluster E1, was more similar to genotypes of sub-cluster E2. This genotype also showed the
354 lower mycelial growth in the *in vitro* assay. It could be hypothesized that this genotype may putatively
355 belong to an additional sub-cluster, since it showed a) several polymorphisms in the ITS region
356 compared to the other Sicilian isolates, b) a peculiar SSR profile, and c) a phenotype different from
357 the others. PCoA also showed the absence of correlation between *L. sulphureus* genotypes and host
358 plants. These findings confirm the results of the single-locus phylogenetic analysis based on ITS and
359 support the hypothesis that *L. sulphureus* genotypes may infect a broad spectrum of host plants.
360 The Spearman's rank correlation test between genetic and geographical pairwise distances showed a
361 significant positive correlation (p-value < 0.05). This outcome, along with the fact that high gene
362 diversity was observed within isolates, may provide evidence that *L. sulphureus* spreads and infects
363 trees through basidiospores, as previously hypothesized (Schwarze, Engels, & Mattheck, 2000) and
364 as documented for other wood decay fungi (Gonthier et al., 2012; Travadon et al., 2012; Sillo et al.,
365 2016).
366 The phenotypic characterization of isolates through the *in vitro* growth assay allowed to distinguish
367 at least four different groups within Sicilian isolates, based on the differences of mycelial growth.
368 Vasaitis et al. (2009) reported that *L. sulphureus* isolates belonging to the cluster E were faster in
369 growth than isolates in cluster C (Vasaitis et al., 2009). In this work, cluster E showed isolate specific
370 variation in mycelial growth rate, suggesting a high phenotypic diversity. The phenotypic diversity
371 within the cluster E was also displayed by differences in the pigmentation of pure cultures (Figure
372 S2). In fact, although no clear differences in the pigmentation among isolates belonging to the two
373 sub-clusters E1 and E2 were observed, pure cultures of Sicilian isolates as a whole ranged from white
374 to yellow-to-orange in colour. The results of the *in vitro* growth assays may mirror the saprotrophic
375 ability of the fungus on wood, as suggested by preliminary results of a growth assay of selected
376 Sicilian isolates on wood substrates (Gianchino, 2017). Interestingly, a significant correlation

between growth on artificial media and on wood substrates has been recently documented for *Armillaria ostoyae* (Romagn.) Herink (Labbé et al., 2017). Phenotypic assays *in vitro* may thus be useful to determine the potential decaying ability of *L. sulphureus* isolates inside the trees, an aspect that may be useful when considering the most appropriate management measures.

No correlation was observed between genetic and phenotypic data in terms of mycelial growth rates *in vitro* (Spearman's rank correlation test, p-value > 0.05). The phenotypic diversity of isolates may be the result of adaptive evolution to the environment mediated by epigenetic changes, as recently demonstrated for other plant pathogens (Dubey & Jeon, 2016). Alternatively, it could be due to genetic polymorphisms affecting loci different from those analysed in this study.

In conclusion, this work allowed us to determine the incidence of *L. sulphureus* on carob in selected areas of Sicily, to develop and use ten SSR markers, specific for *L. sulphureus*, for a precise genotyping of isolates through HRM analysis, and to assess the phenotypic diversity through simple *in vitro* assays. Results showed not only that over one third of carob trees are affected by *L. sulphureus* in the area, but also suggest a risk of transmission of the pathogen from one tree species to another through basidiospores as inferred from data of genetic diversity and on the lack of correlation between fungal genotype and host trees. In addition, the high phenotypic variability observed *in vitro* may reflect a similar variation in natural environment, highlighting the importance of a phenotypic characterization of isolates affecting the trees. From a practical perspective, the pruning/removal of decayed wood, which can serve as substrate for *L. sulphureus* and a source for the emergence of fruiting bodies, could minimize the spread of this wood decay agent in carob orchards.

Acknowledgments

This work was supported by a University of Torino Grant (60%). The authors are grateful to the editors and to the anonymous reviewers for their helpful comments on the manuscript.

References

Banik, M. T., & Burdsall Jr, H. H. (2000). Incompatibility groups among North American populations of *Laetiporus sulphureus* sensu lato. *Mycologia*, *92*, 649–655.

Banik, M. T., Lindner, D. L., Ota, Y., & Hattori, T. (2010). Relationships among North American and Japanese *Laetiporus* isolates inferred from molecular phylogenetics and single-spore incompatibility reactions. *Mycologia*, *102*, 911–917.

Barbagallo, M. G., Di Lorenzo, R., Meli, R., & Crescimanno, F. G. (1997). Characterization of carob germplasm (*Ceratonia siliqua* L.) in Sicily. *Journal of Horticultural Science*, *72*, 537–543.

Barbera, G., & Cullotta, S. (2012). An inventory approach to the assessment of main traditional landscapes in Sicily (Central Mediterranean Basin). *Landscape Research*, *37*, 539–569.

Battle, I., & Tous, J. (1997). Carob tree: *Ceratonia siliqua* L. – Promoting the conservation and use of underutilized and neglected crops. 17. Institute of Plant Genetics and Crop Plant Research, Gatersleben/International Plant Genetic Resources Institute, Rome, Italy.

Bernicchia, A. (2005). Polyporaceae s.l. Ed. Candusso, Alassio, Italy.

Burdsall Jr, H. H., & Banik, M. T. (2001). The genus *Laetiporus* in North America. *Harvard Papers in Botany*, *6*, 43–55.

Dai, Y. C., Cui, B. K., Yuan, H. S., & Li, B. D. (2007). Pathogenic wood–decaying fungi in China. *Forest Pathology*, *37*, 105–120.

429 Distefano, G., Caruso, M., La Malfa, S., Gentile, A., & Wu, S. B. (2012). High resolution melting
430 analysis is a more sensitive and effective alternative to gel–based platforms in analysis of SSR–an
431 example in citrus. *PloS ONE*, *7*, e44202.
432
433 Du, L., Li, Y., Zhang, X., & Yue, B. (2013). MSDB: a user–friendly program for reporting distribution
434 and building databases of microsatellites from genome sequences. *Journal of Heredity*, *104*, 154–
435 157.
436
437 Dubey, A., & Jeon, J. (2016). Epigenetic regulation of development and pathogenesis in fungal plant
438 pathogens. *Molecular Plant Pathology*, *18*, 887–898.
439
440 Franzen, I., Vasaitis, R., Penttilä, R., & Stenlid, J. (2007). Population genetics of the wood–decay
441 fungus *Phlebia centrifuga* P. Karst. in fragmented and continuous habitats. *Molecular Ecology*, *16*,
442 3326–3333.
443
444 Ganopoulos, I., Argiriou, A., & Tsaftaris, A. (2011). Microsatellite high resolution melting (SSR–
445 HRM) analysis for authenticity testing of protected designation of origin (PDO) sweet cherry
446 products. *Food Control*, *22*, 532–541.
447
448 Gardes, M., & Bruns, T. D. (1993). ITS primers with enhanced specificity for basidiomycetes
449 application to the identification of mycorrhizae and rusts. *Molecular Ecology*, *2*, 113–118.
450
451 Gianchino, C. (2017). Incidenza e diversità genetica e fenotipica del fungo lignivoro *Laetiporus*
452 *sulphureus* in carrubeti della Sicilia. Master thesis, University of Bologna, Bologna, Italy.
453
454 Gilbertson, R. L., & Ryvarden, L. (1986). North American polypores 1. Fungiflora, Oslo, Norway.

Giordano, L., Sillo, F., Guglielmo, F., & Gonthier, P. (2015). Comparing visual inspection of trees and molecular analysis of internal wood tissues for the diagnosis of wood decay fungi. *Forestry: An International Journal of Forest Research*, *88*, 465–470.

Gonthier, P., Lione, G., Giordano, L., & Garbelotto, M. (2012). The American forest pathogen *Heterobasidion irregulare* colonizes unexpected habitats after its introduction in Italy. *Ecological Applications*, *22*, 2135–2143.

Gonthier, P., Sillo, F., Lagostina, E., Roccotelli, A., Cacciola, S. O., Stenlid, J., & Garbelotto, M. (2015). Selection processes in simple sequence repeats suggest a correlation with their genomic location: insights from a fungal model system. *BMC Genomics*, *16*, 1107.

Guglielmo, F., Bergemann, S. E., Gonthier, P., Nicolotti, G., & Garbelotto, M. (2007). A multiplex PCR–based method for the detection and early identification of wood rotting fungi in standing trees. *Journal of Applied Microbiology*, *103*, 1490–1507.

Guglielmo, F., Gonthier, P., Garbelotto, M., & Nicolotti, G. (2010). Optimization of sampling procedures for DNA–based diagnosis of wood decay fungi in standing trees. *Letters in Applied Microbiology*, *51*, 90–97.

La Malfa, S., Currò, S., Douglas, A. B., Brugaletta, M., Caruso, M., & Gentile, A. (2014). Genetic diversity revealed by EST–SSR markers in carob tree (*Ceratonia siliqua* L.). *Biochemical Systematics and Ecology*, *55*, 205–211.

Labbé, F., Lung–Escarmant, B., Fievet, V., Soularue, J. P., Laurent, C., Robin, C., & Dutech, C.

(2017). Variation in traits associated with parasitism and saprotrophism in a fungal root–rot pathogen invading intensive pine plantations. *Fungal Ecology*, *26*, 99–108.

Lindner, D. L., & Banik, M. T. (2008). Molecular phylogeny of *Laetiporus* and other brown rot polypore genera in North America. *Mycologia*, *100*, 417–430.

Lindner, D. L., & Banik, M. T. (2011). Intragenomic variation in the ITS rDNA region obscures phylogenetic relationships and inflates estimates of operational taxonomic units in genus *Laetiporus*. *Mycologia*, *103*, 731–740.

Massa, B., & La Mantia, T. (2007). Forestry, pasture, agriculture and fauna correlated to recent changes in Sicily. *Forest@–Journal of Silviculture and Forest Ecology*, *4*, 418.

Maurice, S., Skrede, I., LeFloch, G., Barbier, G., & Kauserud, H. (2014). Population structure of *Serpula lacrymans* in Europe with an outlook to the French population. *Mycologia*, *106*, 889–895.

Milgroom, M. G. (1996). Recombination and the multilocus structure of fungal populations. *Annual Review of Phytopathology*, *34*, 457–477.

Nagy, L. G., Riley, R., Tritt, A., Adam, C., Daum, C., Floudas, D., Sun, H., Yadav, J. S., Pangilinan, J., Larsson, K. H., Matsuura, K., Barry, K., Labutti, K., Kuo, R., Ohm, R. A., Bhattacharya, S. S., Shirouzu, T., Yoshinaga, Y., Martin, F. M., Grigoriev, I. V., & Hibbett, D. S. (2015). Comparative genomics of early–diverging mushroom–forming fungi provides insights into the origins of lignocellulose decay capabilities. *Molecular Biology and Evolution*, *33*, 959–970.

Nazrul, M. I., & YinBing, B. (2011). Differentiation of homokaryons and heterokaryons of *Agaricus*

bisporus with inter-simple sequence repeat markers. *Microbiological research*, *166*, 226–236.

Peakall, P. E., & Smouse, R. (2012). GenAlEx 6.5: genetic analysis in Excel. Population genetic software for teaching and research—an update. *Bioinformatics*, *28*, 2537–2539.

Petrović, J., Glamočlija, J., Stojković, D. S., Ćirić, A., Nikolić, M., Bukvički, D., Guerzoni, M. E., & Soković, M. D. (2013). *Laetiporus sulphureus*, edible mushroom from Serbia: Investigation on volatile compounds, *in vitro* antimicrobial activity and *in situ* control of *Aspergillus flavus* in tomato paste. *Food and Chemical Toxicology*, *59*, 297–302.

Petrović, J., Stojković, D., Reis, F. S., Barros, L., Glamočlija, J., Ćirić, A., Ferreira, I. C., & Soković M. (2014). Study on chemical, bioactive and food preserving properties of *Laetiporus sulphureus* (Bull.: Fr.) Murr. *Food & Function*, *5*, 1441–1451.

Pleszczyńska, M., Wiater, A., Siwulski, M., & Szczodrak, J. (2013). Successful large–scale production of fruiting bodies of *Laetiporus sulphureus* (Bull.: Fr.) Murrill on an artificial substrate. *World Journal of Microbiology and Biotechnology*, *29*, 753–758.

Ramón-Laca, L., & Mabberley, D. J. (2004). The ecological status of the carob–tree (*Ceratonia siliqua*, Leguminosae) in the Mediterranean. *Botanical Journal of the Linnean Society*, *144*, 431–436.

Rogers, S. O., Holdenrieder, O., & Sieber, T. N. (1999). Intraspecific comparisons of *Laetiporus sulphureus* isolates from broadleaf and coniferous trees in Europe. *Mycological Research*, *103*, 1245–1251.

Schwarze, F. W., Engels, J., & Mattheck, C. (2000). Fungal strategies of wood decay in trees.

Springer–Verlag Berlin Heidelberg, Heidelberg, Germany.

Sillo, F., Savino, E., Giordano, L., Girometta, C., Astegiano, D., Picco, A. M., & Gonthier, P. (2016). Analysis of genotypic diversity provides a first glimpse on the patterns of spread of the wood decay fungus *Perenniporia fraxinea* in an urban park in Northern Italy. *Journal of Plant Pathology*, *98*, 617–624.

Sillo, F., Giordano, L., Zampieri, E., Lione, G., De Cesare, S., & Gonthier, P. (2017). HRM analysis provides insights on the reproduction mode and the population structure of *Gnomoniopsis castaneae* in Europe. *Plant Pathology*, *66*, 293–303.

Song, J., & Cui, B. K. (2017). Phylogeny, divergence time and historical biogeography of *Laetiporus* (Basidiomycota, Polyporales). *BMC Evolutionary Biology*, *17*, 102.

Song, J., Chen, Y., Cui, B., Liu, H., & Wang, Y. (2014). Morphological and molecular evidence for two new species of *Laetiporus* (Basidiomycota, Polyporales) from southwestern China. *Mycologia*, *106*, 1039–1050.

Stalpers, J. A. (1978). Identification of wood–inhabiting Aphyllophorales in pure culture. *Studies in Mycology*, *16*, 1–248.

Tamura, K., Stecher, G., Peterson, D., Filipski, A., & Kumar, S. (2013). MEGA6: molecular evolutionary genetics analysis version 6.0. *Molecular Biology and Evolution*, *30*, 2725–2729**.**

Travadon, R., Smith, M. E., Fujiyoshi, P., Douhan, G. W., Rizzo, D. M., & Baumgartner, K. (2012). Inferring dispersal patterns of the generalist root fungus *Armillaria mellea*. *New Phytologist*, *193*,

559 959–969.
560
561 Turkoglu, A., Duru, M. E., Mercan, N., Kivrak, I., & Gezer, K. (2007). Antioxidant and antimicrobial
562 activities of *Laetiporus sulphureus* (Bull.) Murrill. *Food Chemistry*, *101*, 267–273.
563
564 Vannini, A., Contarini, M., Faccoli, M., Valle, M. D., Rodriguez, C. M., Mazzetto, T., Guarneri, D.,
565 Vettraino, A. M., & Speranza, S. (2017). First report of the ambrosia beetle *Xylosandrus compactus*
566 and associated fungi in the Mediterranean maquis in Italy, and new host–pest associations. *EPPO*
567 *Bulletin*, *47*, 100–103.
568
569 Vasaitis, R., Menkis, A., Lim, Y. W., Seok, S., Tomsovsky, M., Jankovsky, L., Lygis, V., Slippers, B.,
570 & Stenlid, J. (2009). Genetic variation and relationships in *Laetiporus sulphureus* s. lat., as
571 determined by ITS rDNA sequences and in vitro growth rate. *Mycological Research*, *113*, 326–336.
572
573 Vasaitis, R. (2013). Heart rots, sap rots and canker rots. In: *Infectious forest diseases*. Ed. by Gonthier,
574 P. & Nicolotti, G. Wallingford: CAB International, pp. 197–229.
575
576 Vasiliauskas, R., Sunhede, S., & Stenlid, J. (2003). Distribution, status and biology of oak polypores
577 in Baltic Sea region. In: *Forest Health Problems in Older Forest Stands. Proceedings of the*
578 *Nordic/Baltic Forest Pathology Meeting, Denmark, September 2002.* Ed. I.M., Thomsen. Danish
579 Forest and Landscape Research Institute, Horsholm, pp. 61–66.
580
581 Wiater, A., Pleszczyńska, M., Szczodrak, J., & Janusz, G. (2012). Comparative studies on the
582 induction of *Trichoderma harzianum* mutanase by α–(1→3)–glucan–rich fruiting bodies and mycelia
583 of *Laetiporus sulphureus*. *International Journal of Molecular Sciences*, *13*, 9584–9598.
584

Xanthopoulou, A., Ganopoulos, I., Koubouris, G., Tsaftaris, A., Sergendani, C., Kalivas, A., & Madesis, P. (2014). Microsatellite high–resolution melting (SSR–HRM) analysis for genotyping and molecular characterization of an *Olea europaea* germplasm collection. *Plant Genetic Resources*, *12*, 273–277.

Zambounis, A., Xanthopoulou, A., Karaoglanidis, G., Tsaftaris, A., & Madesis, P. (2016). A new accurate genotyping HRM method for *Alternaria* species related to fruit rot diseases of apple and pomegranate. *International Journal of Phytopathology*, *4*, 159–165.

Figure legends

FIGURE 1. Map of the sampling area. Gray triangles represent sampled carob trees. Black circles represent locations where fungal fruiting bodies were collected. Map was created and customized by using TileMill (https://tilemill-project.github.io/tilemill/).

FIGURE 2. Phylogenetic tree including ITS sequences of different *Laetiporus* taxa. The sequences were aligned using ClustalW in MEGA v. 6 (Tamura et al., 2013) and the tree (unrooted) was

609 constructed using the Maximum Likehood (ML) method. Numbers indicate bootstrap values. Only
610 taxonomically described *Laetiporus* species were represented. The four undescribed taxa (*Laetiporus*
611 sp.) from South Africa, Hawaii, Costa Rica and Argentina, corresponding to cluster H, I, L and M,
612 respectively, were not included in the tree.
613
614 **FIGURE 3.** Phylogenetic tree including ITS sequences of *Laetiporus sulphureus*. The sequences
615 were aligned using ClustalW in MEGA v. 6 (Tamura et al., 2013) and the tree (unrooted) was
616 constructed using the Maximum Likehood (ML) method. Numbers indicate bootstrap values. For
617 each sequence, information on geographic origin and host tree are provided. Abbreviations: AUS,
618 Austria; CAN, Canada; CZE, Czech Republic; DEN, Denmark; ITA, Italy; LAT, Latvia; LIT,
619 Lithuania; SPA, Spain; SWE, Sweden; URU, Uruguay.
620
621 **FIGURE 4.** Melting curve difference plots after normalization and overlay for the ten polymorphic
622 SSR loci. Differences in terms of relative fluorescence were obtained using the Precision Melt
623 Analysis™ Software. Each curve represent a different allele. (a) Ls_A_345; (b) Ls_AC_322; (c)
624 Ls_ATGCCC11; (d) Ls_CAG_633; (e) Ls_CAG_159; (f) Ls_G_413; (g) Ls_GAG_238; (h)
625 Ls_GCA_174; (i) Ls_GGA_479; (l) Ls_TTC_500.
626
627 **FIGURE 5.** Results of PCoA on genetic data generated by the SSR-HRM genotyping. Gray squares
628 represent isolates belonging to *L. sulphureus* sub-cluster E1, while black diamond represent isolates
629 belonging to sub-cluster E2.
630
631 **FIGURE 6.** Results of PCoA on phenotypic data obtained from the *in vitro* growth assay.
632
633
634

635 **Table 1.** List of *L. sulphureus* isolates used in this study.

Isolate ID Code	Host	Geographic origins	Latitude	Longitude
C1	*Ceratonia siliqua*	Sicily (Italy)	36.89825	14.86479
C2	*Ceratonia siliqua*	Sicily (Italy)	36.92324	14.74267
C3	*Ceratonia siliqua*	Sicily (Italy)	36.89288	14.88271
C4	*Ceratonia siliqua*	Sicily (Italy)	36.94353	14.87465
D1	*Ceratonia siliqua*	Sicily (Italy)	36.92010	14.82380
D3	*Ceratonia siliqua*	Sicily (Italy)	36.94248	14.88063
D4	*Ceratonia siliqua*	Sicily (Italy)	36.91627	14.74451
D5	*Ceratonia siliqua*	Sicily (Italy)	37.02037	14.71584
F1	*Ceratonia siliqua*	Sicily (Italy)	36.91437	14.86937
F2	*Ceratonia siliqua*	Sicily (Italy)	36.81274	14.84336
F3	*Ceratonia siliqua*	Sicily (Italy)	36.94810	14.88038
F4	*Ceratonia siliqua*	Sicily (Italy)	37.04736	14.78326
F5	*Ceratonia siliqua*	Sicily (Italy)	36.92972	14.74760
F6	*Ceratonia siliqua*	Sicily (Italy)	37.13120	14.85319
G1	*Ceratonia siliqua*	Sicily (Italy)	36.92437	14.83428
G2	*Ceratonia siliqua*	Sicily (Italy)	36.92519	14.84561
G3	*Ceratonia siliqua*	Sicily (Italy)	36.94364	14.92788
G4	*Ceratonia siliqua*	Sicily (Italy)	36.93788	14.73893
G5	*Prunus amygdalus*	Sicily (Italy)	36.91716	14.74974
G6	*Ceratonia siliqua*	Sicily (Italy)	36.95976	14.83583
G7	*Ceratonia siliqua*	Sicily (Italy)	36.97077	14.84270
I1	*Ceratonia siliqua*	Sicily (Italy)	36.92116	14.87124
O1	*Ceratonia siliqua*	Sicily (Italy)	36.98445	14.83350
O2	*Ceratonia siliqua*	Sicily (Italy)	36.92574	14.81369
O3	*Ceratonia siliqua*	Sicily (Italy)	36.95476	14.88278
Em-A	*Castanea sativa*	Tuscany (Italy)	-	-
Em-B	*Castanea sativa*	Tuscany (Italy)	-	-
GAIOLA	*Castanea sativa*	Piedmont (Italy)	-	-
VALLERE	*Quercus* sp.	Piedmont (Italy)	-	-

636

637 **Table 2**. SSR markers developed in the study with related allelic diversity. Sequence and ID of
638 primers, number of alleles (Na), number of effective alleles based on their frequencies (Ne) and gene
639 diversity (*h*) *per* SSR locus are shown.
640

Locus	Sequence of the primer	ID primer	Na	Ne	*h*
Ls_ GAG_238	GCAAGGCTAAGGTGTGTCCA	**laets_GAG_238_f**	3	2.129	0.530
	TCCTCTTCCTCTGCCAATTC	**laets_GAG_238_r**			
Ls_ CAG_633	ATATGCCCTCCAATGAGCAG	**laets_GAG_238_r**	5	3.461	0.711
	ATGAACGATCCGTTCTGCAA	**laets_CAG_633_f**			
Ls_GGA_174	TCACGGAGAGCATGAGACTG	**laets_GGA_174_f**	2	1.071	0.067
	GTGTCCATCTCGTCCAGGTT	**laets_GGA_174_r**			
Ls_CGA_159	TCCGCCATTCAACTTAACAA	**laets_CGA_159_f**	7	3.948	0.747
	TGACGTTGTACTCGGATGGA	**laets_CGA_159_r**			
Ls_AC_322	TCAGGTGCACTTTCTGTCCTT	**laets_AC_322_f**	6	3.267	0.694
	GGCTGCTCATCCTGTAGGG	**laets_AC_322_r**			
Ls_A_345	TGAGACTCAGGGGAAGGAGA	**laets_A_345_f**	7	4.918	0.797
	GATTTCCTGAACCCGATAACC	**laets_A_345_r**			
Ls_G_413	TTGAGCAACCTGTTGAGTGG	**laets_G_413_f**	4	3.461	0.711
	GCTCTCTGTTCCGTGTCTCC	**laets_G_413_r**			
Ls_GGA_479	TGAACGTGAGGCAGATCAAG	**laets_GGA_479_f**	3	1.532	0.347
	GCGGTCTCAGCATAAAGTCC	**laets_GGA_479_r**			
Ls_TTC_500	CCCTCAAACGTCTCCACATT	**laets_TTC_500_f**	6	1.566	0.361
	AGAGCGTCAGCAAGGAAGAC	**laets_TTC_500_r**			
Ls_ ATGCCC_111	CACGCTCTGCACTACACCAT	**laets_ATGCCC_111_f**	10	6.622	0.849
	GAGGAGTCCGAGTCATACGAA	**laets_ATGCCC_111_r**			
			Na	**Ne**	***h***
		Average	5.300	3.198	0.581
		Standard Error	0.761	0.543	0.079

641
642

643 **Table 3.** Mycelial radial growth expressed in mm of colonization of agar medium in Petri dishes of
644 Sicilian isolates at different times (days after inoculation). For each isolate, average of measures of
645 the five replicates and standard deviation (SD) are shown.
646

Isolate ID Code	Radius of fungal colony (mm) ± SD			
	After 2 days	After 4 days	After 6 days	After 8 days
C1	4.75±2.24	20.70±2.30	33.60±1.30	38.00±1.22
C2	7.05±2.19	29.50±5.24	38.50±1.29	40.00±0.00*
C3	7.35±1.20	24.90±2.17	39.10±0.90	40.00±0.00*
C4	6.65±4.28	25.90±0.84	37.10±2.26	38.30±1.27
D1	7.30±3.42	32.30±8.96	39.53±0.51	40.00±0.00*
D3	8.10±2.17	28.60±2.17	36.50±2.24	40.00±0.00*
D4	8.25±1.50	30.20±1.52	40.00±0.00*	40.00±0.00*
D5	9.35±1.15	30.20±4.77	40.00±0.00*	40.00±0.00*
F1	5.75±1.46	22.80±1.52	31.60±2.28	37.00±2.55
F2	7.50±1.32	30.20±1.67	40.00±0.00*	40.00±0.00*
F3	5.75±1.00	27.10±1.64	37.90±1.64	40.00±0.00*
F4	6.00±1.06	27.70±2.88	38.70±1.30	40.00±0.00*
F5	7.10±1.52	30.70±4.16	40.00±0.00*	40.00±0.00*
F6	6.35±1.40	27.50±2.92	38.10±3.42	40.00±0.00*
G1	7.85±5.92	28.40±6.30	38.50±1.00	40.00±0.00*
G2	6.05±1.43	27.00±1.22	37.30±2.30	40.00±0.00*
G3	6.75±1.12	26.50±1.58	37.40±2.42	40.00±0.00*
G4	6.65±0.57	27.90±3.03	38.70±0.55	40.00±0.00*
G5	6.55±1.29	25.70±1.52	36.90±0.84	40.00±0.00*
G6	7.85±2.11	27.20±2.70	36.00±1.00	40.00±0.00*
G7	7.50±1.77	30.30±3.78	39.10±0.89	40.00±0.00*

I1	5.05±2.36	27.90±3.27	38.30±1.34	40.00±0.00*
O1	7.15±1.44	26.35±0.45	37.00±2.55	40.00±0.00*
O2	9.80±2.27	31.60±1.92	40.00±0.00*	40.00±0.00*
O3	11.05±0.55	38.30±2.00	40.00±0.00*	40.00±0.00*

*fully-grown culture

650 FIG. 1

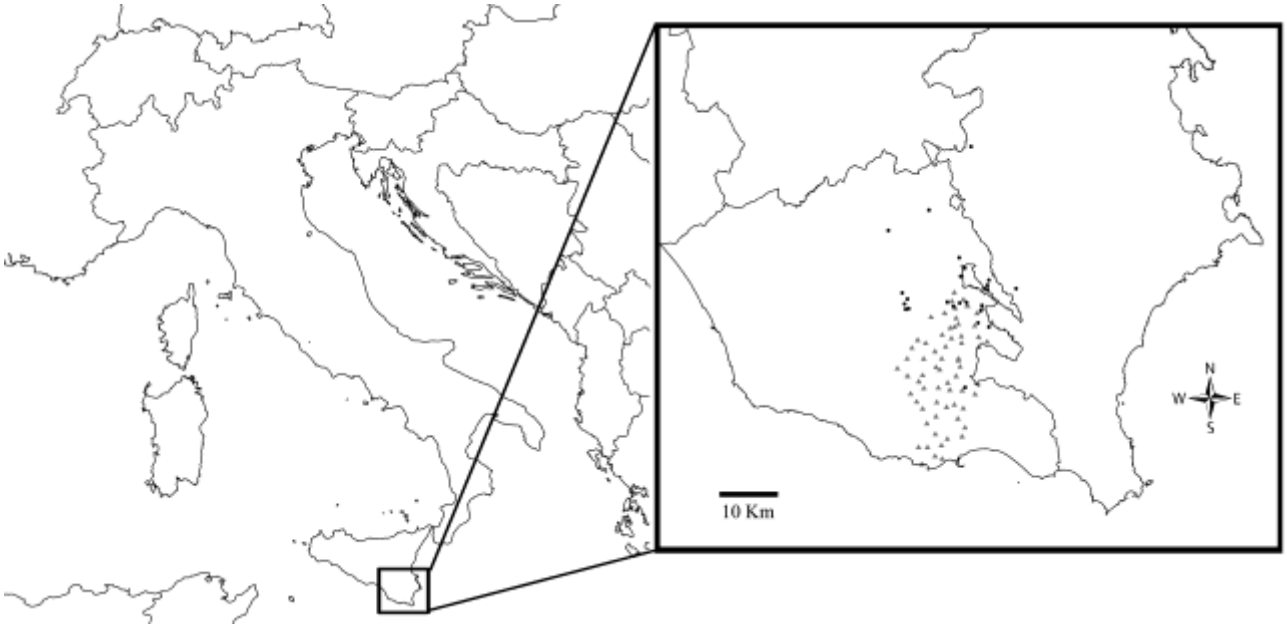

651

652

653 FIG. 2

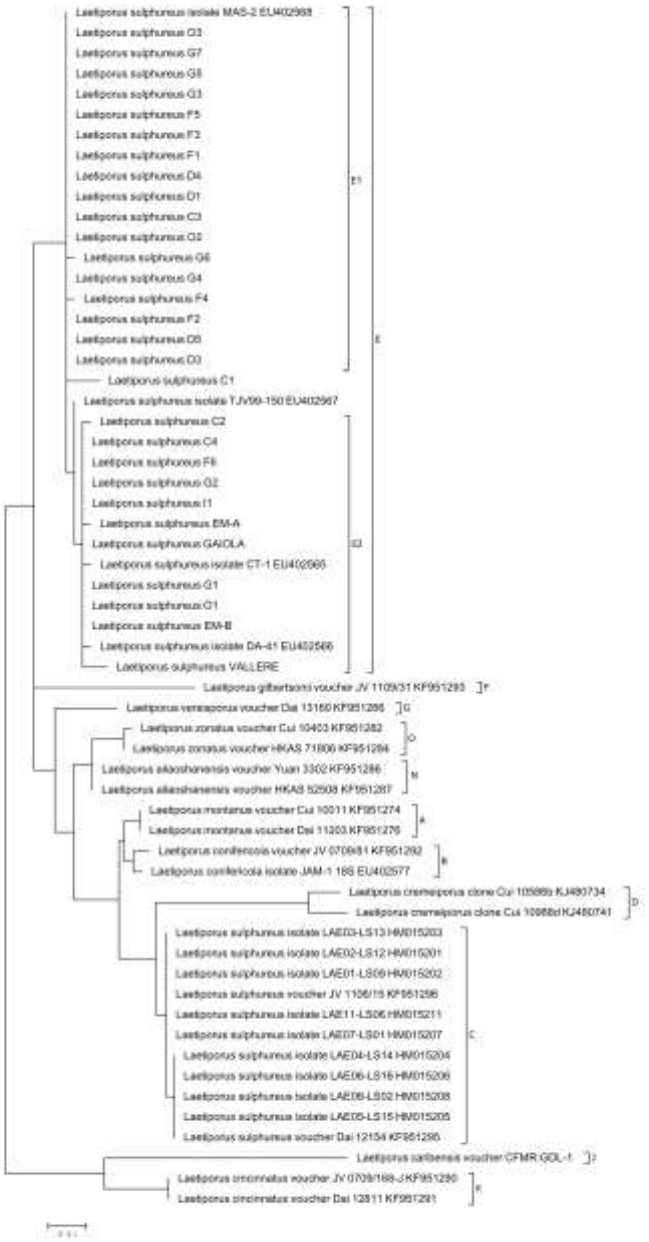

654

655

656

657 FIG. 3

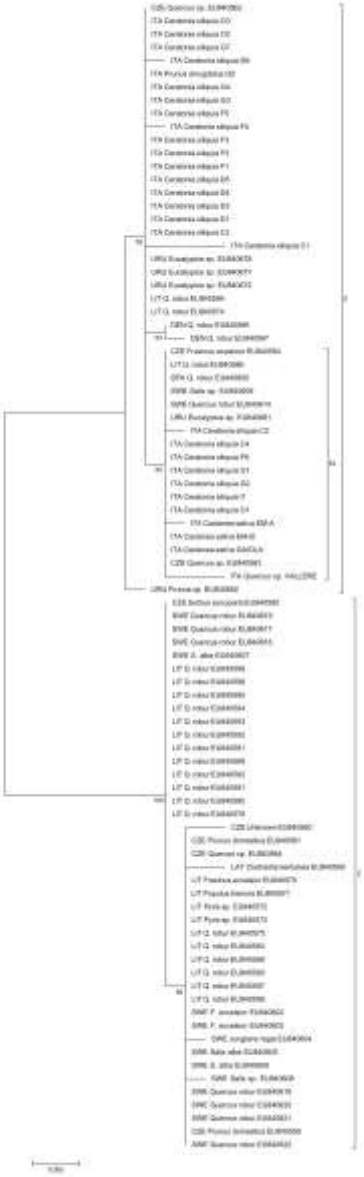

658

659

660

661 FIG. 4

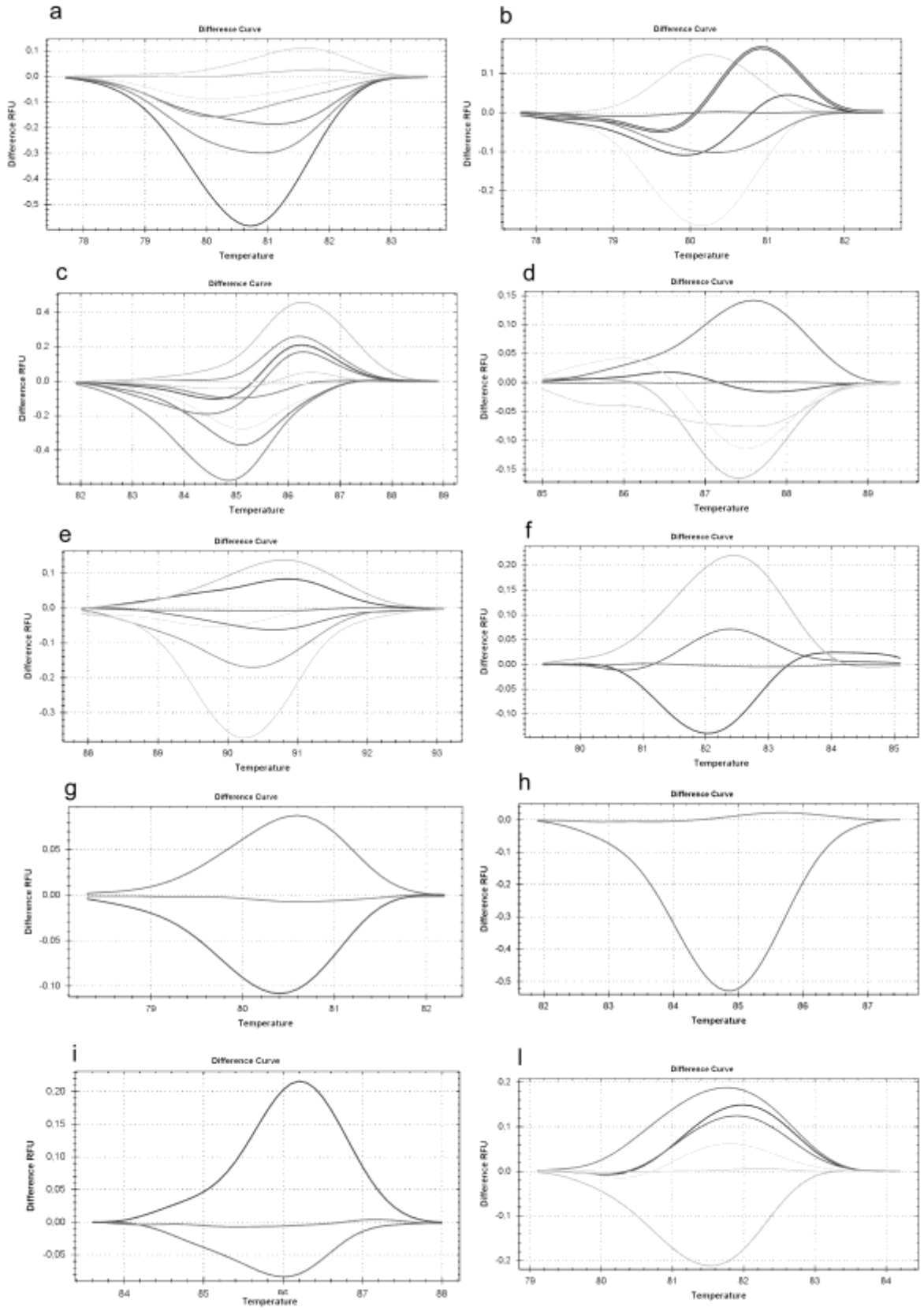

662

663

664 FIG. 5

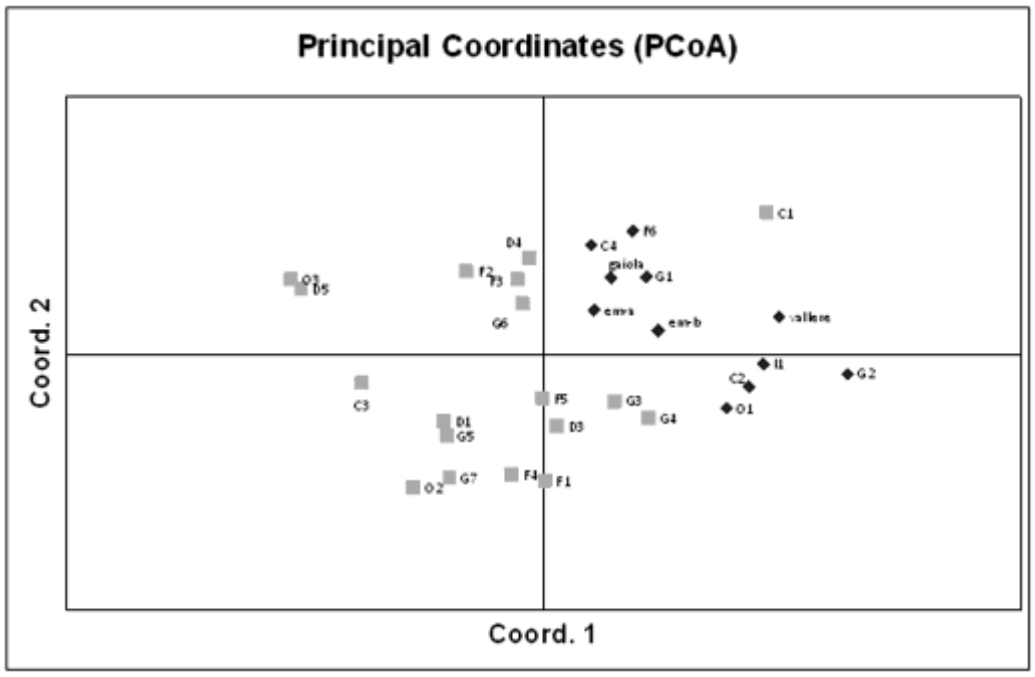

665

666

667 FIG. 6

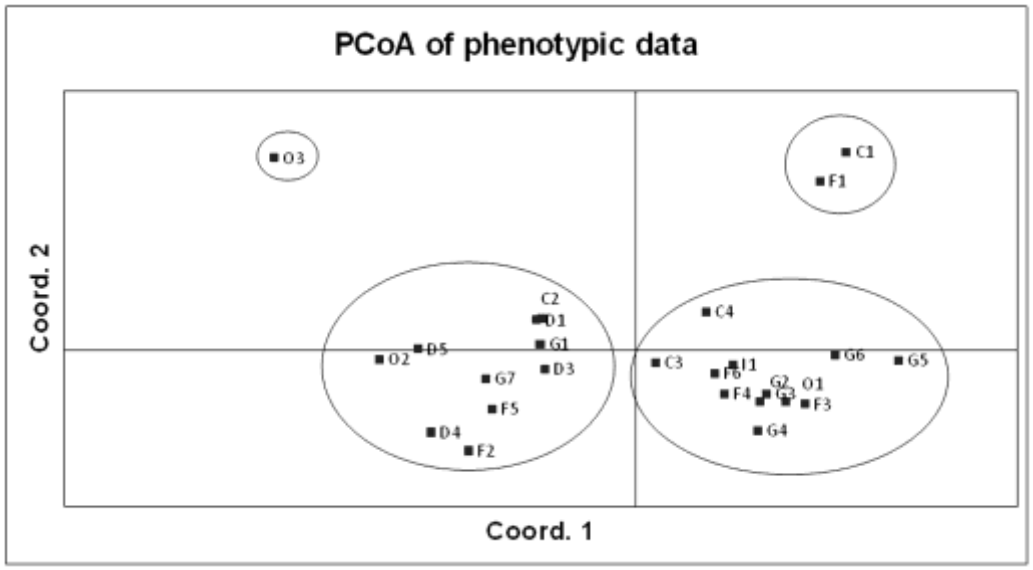

668

669

670